M. Sznaier and O. Camps: A Hankel operator approach to texture modelling and inpainting. In *Texture 2005: Proceedings of the 4th International Workshop on Texture Analysis and Synthesis*, pp. 125–130, 2005.

A Hankel Operator Approach to Texture Modelling and Inpainting

Mario Sznaier Octavia Camps
Department of Electrical Engineering
The Pennsylvania State University
University Park, PA 16802

Abstract— **In this paper we propose a Hankel operator based approach to the problems of texture modelling and inpainting. The main idea is to model textured images as the output of an unknown, periodic, linear shift invariant operator in response to a suitable input. The main result of the paper shows that this operator can be found by factoring a Hankel matrix constructed from the image data. As we illustrate in the paper, the resulting operator can then be applied to a given partial image to reconstruct missing portions, find textons, or synthesize textures from the same family.**

I. Introduction

This paper considers the problems of texture modelling and synthesis. Surveys of the field and extensive references can be found for instance in [11], [26], [20], [24], [30].

Earlier work on texture modelling was based on the use k^{th} order statistics [15], [12]. Most recent statistical approaches use either Markov random fields [6], [18], [5], [29], [10] or multiscale multiple linear kernels at different scales and orientations followed by a non-linear procedure [4], [22], [2], [14], [21], [23], [31].

Texture synthesis algorithms can be classified as *procedural,* based on the statistical approaches described above, or *image-based*, based on stitching pixels or patches from a sample image (see for instance [8], [9], [27], [13], [1], [25], [28], [17]).

The approach that we pursue in this paper is related to previous statistical approaches in the sense that we will also model images exhibiting a given texture as realizations of a second order stationary stochastic process. Motivated by the work in [7] on dynamic texture[1] we will model the intensity values $\mathcal{I}(k,:)$ of the k^{th} row of the image as the output, at step k, of a discrete linear shift-invariant, not necessarily causal, system driven by white noise. In this context, texture modelling can be recast into the problem of identifying a system model with the appropriate properties from the given images. In the first portion of this paper we develop an SVD based algorithm, that allows for extracting texture models from images in an efficient way. In the second portion of the paper we show that these models allow for reducing the problems of finding textons and texture inpainting to a rank minimization problem.

This work was supported in part by AFOSR grant FA9550-05-1-0437 and NSF grants IIS–0117387, ECS–0221562 and ITR–0312558.

[1]Dynamic textures are image sequences of moving scenes with texture such as flowing water, drifting smoke, etc.

II. Notation

$\mathbf{x}$	column vector.
$\mathbf{x}^H$	Hermitian conjugate of $\mathbf{x}$.
$\mathbf{I}_p$	$p \times p$ Identity Matrix
$A(k,:)$	k^{th} (block) row of matrix A
$\sigma_i(\mathbf{A})$	singular values of $\mathbf{A}$.
$\bar{\sigma}(\mathbf{A})$	maximum singular value of $\mathbf{A}$.
$\mathcal{E}(.)$	expected value.
$\mathcal{H}^n$	set of all block circulant Hankel matrix of the form:

$$\mathbf{H}^n = \begin{bmatrix} \mathbf{h}_1 & \mathbf{h}_2 & \dots & \mathbf{h}_n \\ \mathbf{h}_2 & \mathbf{h}_3 & \dots & \mathbf{h}_1 \\ \vdots & \vdots & \ddots & \vdots \\ \mathbf{h}_n & \mathbf{h}_1 & \dots & \mathbf{h}_{n-1} \end{bmatrix}$$

where $\mathbf{h} \in R^{p \times m}$

In the sequel, we will represent a linear system $\mathcal{G}$ by its convolution kernel $\{\mathbf{g}_i\}$. Causal systems (i.e $\mathbf{g}_i = 0,\ i < 0$) will also be represented by a state–space realization:

$$\begin{aligned} \mathbf{x}_{k+1} &= \mathbf{A}\mathbf{x}_k + \mathbf{B}u_k \\ y_k &= \mathbf{C}\mathbf{x}_k + \mathbf{D}u_k. \end{aligned} \tag{1}$$

where $\mathbf{x}$, $\mathbf{u}$, and $\mathbf{y}$ represent the states, inputs and outputs, respectively. The two representations are related by:

$$\mathbf{g}_o = \mathbf{D},\ \mathbf{g}_i = \mathbf{C}\mathbf{A}^{i-1}\mathbf{B}, i \geq 1$$

In the sequel, we will associate to any finite sequence $x = \{\mathbf{x}_k\}$, the following circulant Hankel matrix:

$$\mathbf{H}_x^n = \begin{bmatrix} \mathbf{x}_1 & \mathbf{x}_2 & \dots & \mathbf{x}_n \\ \mathbf{x}_2 & \mathbf{x}_3 & \dots & \mathbf{x}_1 \\ \vdots & \vdots & \ddots & \vdots \\ \mathbf{x}_n & \mathbf{x}_1 & \dots & \mathbf{x}_{n-1} \end{bmatrix}.$$

Finally, given a system $\mathcal{G}$, we will denote by $\mathbf{H}_{\mathbf{g}}^n$ the circulant Hankel matrix associated with $\{\mathbf{g}_i\}$.

III. Texture Modelling.

Our starting point is to model the intensity values $\mathcal{I}(k,:)$ of the k^{th} row of the $n \times m$ textuted image as the output, at step k, of a linear system $\mathcal{G}$ driven by white noise u:

$$\mathcal{I}(k,:) = \sum_{\substack{j=1 \\ j \neq k}}^{n} a_{k-j}\mathcal{I}(j,:) + b_{k-j}u_j \tag{2}$$

where a_i, b_i are the unknown parameters to be extracted from the image. A difficulty here is that the unknown operator in not necessarily causal since $\mathcal{I}(k,:)$ in eq. (2) depends on the values of the pixels in all rows, not just those on the rows $\mathcal{I}(j,:),\ j < k$. This issue will be addressed by considering the given $n \times m$ image as one period of an infinite 2D signal with period (n, m). Thus, at any given location (i, j) in the image, the intensity values $\mathcal{I}(r, s)$ at other pixels are available also at position $(r - qn, s - qm)$, and the integer q can always be chosen so that $r - qn < i, s - qm < j$. From this observation, it follows that the unknown system $\mathcal{G}$ can always be chosen to be causal, subject to the additional periodicity constraint, and thus it admits a state–space realization of the form:

$$\begin{aligned} \mathbf{x}_{k+1} =& \mathbf{A}\mathbf{x}_k + \mathbf{B}u_k,\ \mathbf{A}^n = \mathbf{I} \\ \mathbf{y}_k =& \mathbf{C}\mathbf{x}_k. \end{aligned} \tag{3}$$

where for each k, $\mathbf{x}_k$ and u_k represent the state and (unknown) stochastic input, and where the output vector $\mathbf{y}_k \in R^m$ contains all the intensity values $\mathcal{I}(k, l),\ 1 \leq l \leq m$ of the pixels in the k^{th} row of the image. Here the condition $\mathbf{A}^n = \mathbf{I}$ is just a restatement of the periodicity constraint. Finally, note that since this condition implies that $\mathbf{A}^k = \mathbf{A}^{k+n}$, it follows that the effect of an input $\mathbf{u}$ applied at k, is identical to the effect of the same input applied at $k - n$. Thus, without loss of generality it can be assumed that the input u in eq. (3) is non–zero only in the interval $[-(n-1), 0]$. In this context, the modelling problem becomes that of extracting the matrices $\mathbf{A}, \mathbf{B}, \mathbf{C}$ of the model (3) from (possibly noisy) images where $\mathbf{y}_k = \mathcal{I}(k,:)^T + \mathbf{v}_k$ and where only a spectral characterization of the measurement noise $\mathbf{v}$ is available.

IV. Extracting texture models from images.

In this section we present an algorithm for extracting the model parameters from noisy images. This algorithm is based on the SVD of a circulant Hankel matrix constructed from the image data. The first step is to consider a deterministic equivalent of (3), where the stochastic input u and measurement noise $\mathbf{v}$ are replaced by deterministic equivalents satisfying:

$$\begin{aligned} \mathbf{H}_u^T \mathbf{H}_u =& \ \mathbf{I} \\ \bar{\sigma}(\mathbf{H}_\mathbf{v}) \leq& \ \epsilon \end{aligned} \tag{4}$$

where $\mathbf{H}_u$ and $\mathbf{H}_\mathbf{v}$ denote the Hankel matrices associated with the sequences u and v respectively.

Remark 1: It can be shown that, for an ergodic process $\mathbf{z}$, the (i, j) element of $\mathbf{H}_\mathbf{z}^T \mathbf{H}_\mathbf{z}$ is an estimate of the autocorrelation function $\mathcal{R}_\mathbf{z}(i-j)$. Thus, the first condition in (4) is equivalent to imposing that u is a white sequence, while the second forces $\mathbf{v}$ to have a power spectral density bounded by ϵ^2.

With these assumptions, the k^{th} row of the image, $\mathbf{R}_k$, is given by the output at the index k of the system (3) to the input $u_i,\ i \in [-(n-1), 0]$, corrupted by measurement noise $\mathbf{v}_k$, that is:

$$\mathbf{R}_k^T = \sum_{i=-(n-1)}^{0} \mathbf{g}_{k-i} u_i + \mathbf{v}_k$$

where $\mathbf{g}_i = \mathbf{C}\mathbf{A}^{i-1}\mathbf{B}$, or, in matrix form:

$$\mathbf{H}_\mathbf{R} = \mathbf{H}_\mathbf{g} \mathbf{H}_u + \mathbf{H}_\mathbf{v}. \tag{5}$$

Thus, given an image, the corresponding model can be found by (i) first factoring the associated Hankel matrix $\mathbf{H}_\mathbf{R}$ into the form above, subject to the constraints (4) and the periodicity constraint $\mathbf{g}_i = \mathbf{g}_{i+n}$, or equivalently, $\mathbf{A}^n = \mathbf{I}$; and (ii) extracting the matrices $\mathbf{A}, \mathbf{B}, \mathbf{C}$ from $\mathbf{H}_\mathbf{g}$. In general, this problem is not trivial, since approximations of Hankel matrices do not necessarily preserve the Hankel structure. However, in the case under consideration here, the block circulant structure of the matrices can be exploited to obtain a simple factorization algorithm based on a SVD decomposition as follows:

Algorithm 1:

1.- Given an $n \times m$ image, let $\mathbf{R}_i^T$ denote its i^{th} row, and form the $nm \times n$ block circulant matrix:

$$\mathbf{H}_\mathcal{I} \doteq \begin{bmatrix} \mathbf{R}_1 & \mathbf{R}_2 & \dots & \mathbf{R}_n \\ \mathbf{R}_2 & \mathbf{R}_3 & \dots & \mathbf{R}_1 \\ \vdots & \vdots & \ddots & \vdots \\ \mathbf{R}_n & \mathbf{R}_1 & \dots & \mathbf{R}_{n-1} \end{bmatrix}. \tag{6}$$

Select any matrix $\mathbf{H}_u \in \mathcal{H}$ such that $\mathbf{H}_u^T \mathbf{H}_u = \mathbf{I}$, and define:

$$\mathbf{Y} \doteq \mathbf{H}_\mathcal{I} \mathbf{H}_u^T \tag{7}$$

2.- Perform a singular value decomposition:

$$\mathbf{Y} = \begin{bmatrix} \mathbf{U} & \mathbf{U}_\perp \end{bmatrix} \begin{bmatrix} \mathbf{S} & \mathbf{0} \\ \mathbf{0} & \mathbf{0} \end{bmatrix} \begin{bmatrix} \mathbf{V}^T \\ \mathbf{V}_\perp^T \end{bmatrix}, \\ \mathbf{S} = \text{diag}(\sigma_1, \dots, \sigma_n),\ \sigma_i \geq \sigma_j,\ i \geq j \tag{8}$$

3.- Let

$$r = \min\{n, i \colon \sigma_i \leq \epsilon\} \tag{9}$$

and form the rank r matrix

$$\mathbf{H}_r \doteq \mathbf{U}_r \mathbf{S}_r \mathbf{V}_r^T \tag{10}$$

where $\mathbf{S}_r = \text{diag}(\sigma_1, \dots, \sigma_r)$ and $\mathbf{U}_r, \mathbf{V}_r$ denote the submatrices formed by the first r columns of $\mathbf{U}$ and rows of $\mathbf{V}^T$, respectively.

4.- Form the following state space realization:

$$\begin{aligned} \mathbf{A}_r &= \mathbf{S}_r^{-\frac{1}{2}} \mathbf{U}_r^T \mathbf{P}_L \mathbf{U}_r \mathbf{S}_r^{\frac{1}{2}},\ \mathbf{B}_r = \mathbf{S}_r^{\frac{1}{2}} \mathbf{V}_r^{(1)} \\ \mathbf{C}_r &= \mathbf{U}_r^{(1)} \mathbf{S}_r^{\frac{1}{2}} \end{aligned} \tag{11}$$

where

$$\mathbf{P}_L = \begin{bmatrix} 0 & \mathbf{I}_n & 0 & \dots & 0 \\ 0 & 0 & \mathbf{I}_n & \dots & 0 \\ \vdots & \vdots & \ddots & \vdots & \\ \mathbf{I}_n & 0 & 0 & \dots & 0 \end{bmatrix} \tag{12}$$

and where $\mathbf{U}_r^{(1)}$ and $\mathbf{V}_r^{(1)}$ denote the first $n \times r$ block of $\mathbf{U}_r$ and $r \times m$ block of $\mathbf{V}_r^T$, respectively.

Theorem 1: The model $(\mathbf{A}_r, \mathbf{B}_r, \mathbf{C}_r)$ generated by the algorithm above satisfy the following properties:

(i) $\mathbf{A}_r^n = \mathbf{I}$

(ii) There exists some admissible measurement noise $\mathbf{v}$ with $\bar{\sigma}(\mathbf{H_v}) \leq \epsilon$ such that the output of the system:

$$\begin{aligned} \mathbf{x}_{k+1} =& \mathbf{A}_r \mathbf{x}_k + \mathbf{B}_r u_k, \\ \mathbf{y}_k =& \mathbf{C}_r \mathbf{x}_k \end{aligned} \tag{13}$$

in response to an initial condition $\mathbf{x}_{-(n-1)} = \mathbf{0}$ and input:

$$u_{1-k} = \begin{cases} \mathbf{H}_u(k,1) & k = 1, n \\ 0 & \text{otherwise} \end{cases} \tag{14}$$

satisfies $\mathbf{R}_k^T = \mathbf{y}_k + \mathbf{v}_k$, $k = 1, \ldots, n$. That is, the output of the system recreates the image within the measurement noise bounds.

Proof: Given in the Appendix ■

Remark 2: Note that any choice of $\mathbf{H}_u$ yields a model that recreates the texture. Thus, in the absence of additional information, one can always choose $\mathbf{H_u} = \mathbf{I}$.

V. Application 1: Finding Textons

Consider the problem of finding "textons" in an image, that is, subimage that, when tiled, reproduces the original image. Assuming that at least one full period is available in the sample image, in the context discussed above, the problem becomes that of jointly identifying a model and its corresponding period. As we show next, this problem can be solved by finding regions of the image corresponding to local minima of the rank of the associated Hankel matrices.

Finding Textons as a Minimal Rank Problem: Given an $n \times m$ image $\mathcal{I}(x,y)$, let $\mathbf{H}_\mathcal{I}$ denote the associated Hankel matrix. Finally, denote by $(\mathbf{A}, \mathbf{B}, \mathbf{C})$ the state–space matrices of the corresponding model, and assume that the image $\mathcal{I}$ contains at least one complete texton, that is, there exists some $r < \min\{m, n\}$, such that $\mathbf{R}_i = \mathbf{C}\mathbf{A}^{i-1}\mathbf{B}$, with $\mathbf{A} \in R^{r \times r}$, $\mathbf{A}^r = \mathbf{I}$ and $\mathbf{A}^k \neq \mathbf{I}$ for any $1 \leq k < r$ (that is r is the size of the smallest texton). Consider first an *ideal image*, uncorrupted by noise. In this case, from section IV it follows that the following matrix:

$$\mathbf{H}_{Nr} \doteq \begin{bmatrix} \mathbf{R}_1 & \mathbf{R}_2 & \ldots & \mathbf{R}_{Nr} \\ \mathbf{R}_2 & \mathbf{R}_3 & \ldots & \mathbf{R}_1 \\ \vdots & \vdots & \ddots & \vdots \\ \mathbf{R}_{Nr} & \mathbf{R}_1 & \ldots & \mathbf{R}_{Nr-1} \end{bmatrix}. \tag{15}$$

where N denotes the number of complete textons contained in the sample image, has rank r, since it can be written as the product of two rank r matrices:

$$\begin{aligned} &\mathbf{H}_{Nr} = \mathcal{O}\mathcal{C} \\ &\quad \mathcal{C} = \begin{bmatrix} \mathbf{B} & \mathbf{AB} & \ldots & \mathbf{BA}^{Nr} \end{bmatrix} \\ &\quad \mathcal{O} = \begin{bmatrix} \mathbf{C}^T & \mathbf{A}^T\mathbf{C}^T & \ldots & (\mathbf{A}^{Nr})^T\mathbf{C}^T \end{bmatrix}^T \end{aligned} \tag{16}$$

On the other hand, for any $1 \leq k \leq r-1$, the matrix

$$\mathbf{H}_{n_k} \doteq \begin{bmatrix} \mathbf{R}_1 & \mathbf{R}_2 & \ldots & \mathbf{R}_{n_k} \\ \mathbf{R}_2 & \mathbf{R}_3 & \ldots & \mathbf{R}_1 \\ \vdots & \vdots & \ddots & \vdots \\ \mathbf{R}_{n_k} & \mathbf{R}_1 & \ldots & \mathbf{R}_{n_k-1} \end{bmatrix} \tag{17}$$

where $n_k \doteq (N-1)r + k$, satisfies $\text{rank}(\mathbf{H}_{(N-1)r+k}) > r$, since otherwise this implies $\mathbf{A}^{(N-1)r+k} = \mathbf{I}$, which together with $\mathbf{A}^r = \mathbf{I}$ implies $\mathbf{A}^k = \mathbf{I}$, against the hypothesis that r was the size of the smallest texton. Thus, in the case of *ideal* images, textons can be found by considering a sequence of Hankel matrices of the form (6), starting with $k = n$, with decreasing values of k, and searching for relative minima of $\text{rank}(\mathbf{H}_k)$.

Consider now the more realistic case of ideal texture, corrupted by additive noise $\mathbf{v}$. In this case, the Hankel matrices of the actual $(\mathbf{Y}_k)$ and ideal $(\mathbf{H}_k)$ images are related by

$$\mathbf{Y}_k = \mathbf{H}_k + \mathbf{H_v}$$

and thus the problem becomes

$$\min_k \{r\} \text{ subject to: } \begin{cases} \bar{\sigma}(\mathbf{H_v}) = \bar{\sigma}(\mathbf{Y}_k - \mathbf{H}_k) \leq \epsilon \\ \mathbf{H}_k \in \mathcal{H}, \ \text{rank}(\mathbf{H}_k) = r \end{cases} \tag{18}$$

precisely the type of problem solved by Algorithm 1 (see Corollary 1 in the Appendix).

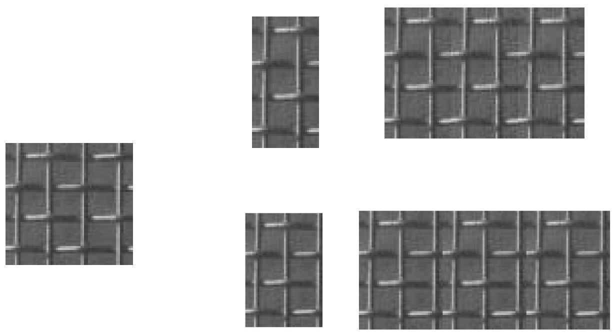

original image texton expanded image

Fig. 1. Finding textons as a rank minimization problem. Top: Rank Minimization. Bottom: Existing approach (Correlation Maximization)

This approach is illustrated in Figure 1 where it was used to (i) find a texton, (ii) extract the corresponding model, and (iii) expand the original image. For comparison, an algorithm based on finding the peak of the autocorrelation function [16], fails to identify the correct periodicity, as shown in the bottom half of Figure 1. Additional examples of identifying textons by searching for minimal rank Hankel matrices are shown in Figure 2.

VI. Application 2: Texture Inpainting

Consider now the problem of *restoring* a textured image where some pixels are missing. Formally, given an image

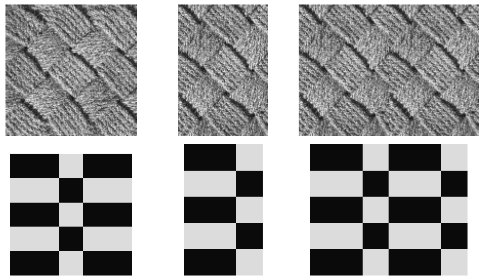

Fig. 2. Additional examples of finding textons through rank minimization.

$\mathcal{I}(x,y)$ and a set of indexes of missing pixels $\mathcal{S} = \{(i_1,j_1),\ldots,(i_s,j_s)\}$, the goal is to determine the intensity values $\mathcal{I}(i,j); (i,j) \in \mathcal{S}$ that best fit, in some sense, the rest of the image. As we show next, this problem can be recast into a rank minimization problem.

Restoration as a Rank Minimization Problem: As before, given an $n \times m$ image $\mathcal{I}(x,y)$, let $\mathbf{H}$ and $(\mathbf{A},\mathbf{B},\mathbf{C})$ denote the associated Hankel matrix and state–space model, respectively. Assume that the image $\mathcal{I}$ contains at least one complete period, that is $\mathbf{A} \in R^{r\times r}$, with $\mathbf{A}^r = \mathbf{I}$ and $r < \min\{m,n\}$.

Consider now the situation where a portion of the image is missing. As we show next, this missing portion can be recovered by minimizing the rank of $\mathbf{H}$, provided that enough information is left in the image to recover at least one period. (Note that this information does not have to be necessarily contiguous). Start by considering an *ideal, noiseless* image, containing an integer number of periods (this assumption will be removed later). Assume now that $\mathbf{R}_1$, the first row of the image, is missing or corrupted. The corresponding Hankel matrix is given by:

$$\mathbf{H}(\mathbf{x}) \doteq \begin{bmatrix} \mathbf{x} & \mathbf{R}_r & \ldots & \mathbf{R}_1 & \ldots & \mathbf{R}_2 \\ \mathbf{R}_2 & \mathbf{x} & \ldots & \mathbf{R}_2 & \ldots & \mathbf{R}_1 \\ \vdots & \vdots & \ddots & \vdots & \ldots & \vdots \\ \mathbf{R}_1 & \mathbf{R}_r & \ldots & \mathbf{x} & \ldots & \mathbf{R}_r \\ \vdots & \vdots & \ldots & \vdots & \ddots & \vdots \\ \mathbf{R}_r & \mathbf{R}_{r-1} & \ldots & \mathbf{R}_r & \ldots & \mathbf{x} \end{bmatrix} \quad (19)$$

where $\mathbf{x}$ denotes the missing pixels. Let $(r_o, \mathbf{x}_o)$ denote the solution to the rank minimization problem $r_o = \min_{\mathbf{x}} \text{rank}\{\mathbf{H}(\mathbf{x})\}$. Since by assumption the image contains at least one full period, and the minimal realization of this period requires r states, it follows that $\mathbf{H}(\mathbf{x})$ contains at least one rank r submatrix $\mathbf{M}_r = [\mathbf{R}_{j_i}]$. Hence $r_o \geq r$ and the minimum can be achieved for instance when $\mathbf{x}_o$ is set to the correct value. Thus, for any minimizing solution $\tilde{\mathbf{x}}$, there exist r columns $\mathbf{H}(:,i)$ and scalars α_i such that $\mathbf{H}(:,1) = \sum_{i=1}^{r} \alpha_i \mathbf{H}(:,i)$. By contradiction, assume now that $\tilde{\mathbf{x}} \neq \mathbf{R}_1$. Since all indexes i appear in $\mathbf{H}(:,1)$, this implies, (by selecting an appropriate subset of rows of $\mathbf{H}$), that $\mathbf{R}_1 = \sum_{i=1}^{r-1} \beta_i \mathbf{R}_i$, for some β_i not all zero, which contradicts the hypothesis that $\text{rank}(\mathbf{M}_r) = r$.

In the case of real images, corrupted by noise, let $\mathbf{Y}(\mathbf{x})$ and $\mathbf{H}_g$ denote the corresponding image and the underlying low rank Hankel operator. From the reasoning above, it follows that the missing pixels $\mathbf{x}$ can be found by solving the following problem:

$$\min_{\mathbf{x}}\{r\} \text{ subject to: } \begin{cases} \bar{\sigma}(\mathbf{Y}-\mathbf{H}) \leq \epsilon \\ \mathbf{H} \in \mathcal{H},\ \text{rank}(\mathbf{H}) = r \end{cases} \quad (20)$$

Direct application of Corollary 1 in the Appendix leads to the following equivalent (non–convex) optimization problem:

$$\min_{\mathbf{x}}\{r\} \text{ subject to:} \sigma_i(\mathbf{x}) \leq \epsilon, i \geq r$$

where $\sigma_i(.)$ denote the singular values of $\mathbf{Y}$, in decreasing order.

Finally, the case where the image does not contain an integer number of periods can be solved by combining the idea above with the technique proposed for finding textons: A sequence of rank minimization problems can be solved, for submatrices of increasing dimensions. The texton and missing pixels can be jointly determined by finding the region, along with the corresponding minimizer $\mathbf{x}_o(\mathcal{T})$ that minimizes $\text{rank}[\mathbf{H}(\mathbf{x},\mathcal{T})]$. Note also that the proofs above generalize to other regions as long as the hypothesis that $\mathbf{H}$ contains a rank r submatrix holds.

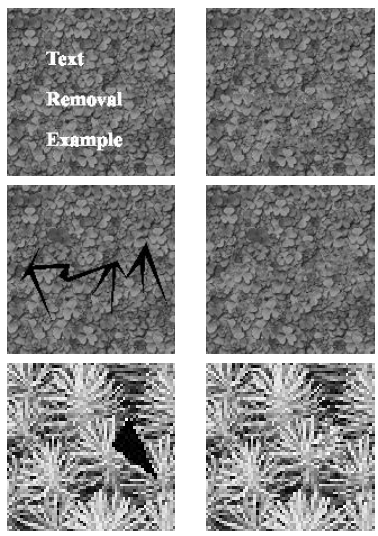

Fig. 3. Corrupted and Restored Images

Reducing the Computational Complexity: A potential difficulty with the approach outlined above stems from the fact that rank minimization problems are known to be generically NP–hard [3]. However, as we briefly show in the sequel, in this case the specific structure of the problem can be exploited to obtain computationally tractable convex relaxations. Begin by noting that if the Hankel matrix (19) has rank r, so does the Toeplitz matrix:

$$\mathbf{T}(\mathbf{x}) \doteq \begin{bmatrix} \mathbf{R}_1 & \mathbf{x} & \dots & \mathbf{R}_{n-1} \\ \mathbf{R}_2 & \mathbf{R}_1 & \dots & \mathbf{x} \\ \vdots & \vdots & \ddots & \vdots \\ \mathbf{x} & \mathbf{R}_{n-1} & \dots & \mathbf{R}_1 \end{bmatrix} \quad (21)$$

(this can be easily shown by noting that $\mathbf{H}^T\mathbf{H} = \mathbf{T}^T\mathbf{T}$). Moreover, it is not hard to show that the singular values of $\mathbf{T}$ are given by the magnitude of the Fourier Transform of its first column, evaluated at the frequencies $\omega_i = \frac{2\pi i}{n}$, $i = 0, 1, \dots, n-1$, that is:

$$\sigma(i) = \left[F^H(\omega_i)F(\omega_i)\right]^{\frac{1}{2}}, \; F(\omega_i) \doteq \sum_{k=1,n} \mathbf{R}_k e^{j(k-1)\omega_i}$$

Since $\mathbf{T}$ is an affine function of the missing pixels $\mathbf{x}$, it follows that $\sigma(i)$ is a convex function of $\mathbf{x}$. One can then attempt to solve Problem (20) by solving the following optimization problem:

$$\min_{\mathbf{x}} \sum_i log(\sigma(i)^2 + \epsilon) \quad (22)$$

The idea behind this function is to drive as many singular values as possible below the noise threshold ϵ. Consistent numerical experience shows that this relaxation achieves a value of the rank within 1 to 2% of the actual minimum.

The use of this relaxation is illustrated in Figure 3, where it was used to remove unwanted text and to restore missing pixel values.

VII. Conclusions

This paper approaches the problems of texture analysis and synthesis from an operator theoretic viewpoint, where images exhibiting a given texture are viewed as the output, corrupted by noise, of an unknown operator with periodic impulse response to a suitable input.

Motivated by existing subspace identification methods and their relationship with well known results in realization theory, we address the problem of extracting models from textured images, by working directly with a *circulant* Hankel matrix $\mathbf{H}_{\mathcal{I}}$ constructed from the image pixels $\mathcal{I}(i, j)$. The main result of the paper shows that a state–space realization model of a given texture can be obtained directly from a SVD–decomposition of $\mathbf{H}_{\mathcal{I}}$. This result was established by noting that rank–constraint approximations obtained by truncating the SVD decomposition of a circulant Hankel matrix automatically inherit the Hankel structure, and that the periodicity constraint induces a circulant structure on the Hankel operator modelling the texture.

The proposed modelling approach was illustrated with two applications: (i) finding textons and (ii) texture inpainting, that is, to seamlessly complete a textured image with missing pixels. As we show in the paper, both problems are related to the rank of $\mathbf{H}_{\mathcal{I}}$. The first problem entails finding regions of the image associated with relative minima of the rank of the corresponding Hankel matrix, while the second leads to a rank–minimization problem. While these problems are known to be generically NP–hard, in this case the properties of circulant Hankel matrices can be exploited to obtain tight convex relaxations.

It is also worth mentioning that the algorithms proposed here can be modified to incorporate time evolution of the state representation, potentially providing for efficient ways of modelling and recognizing dynamic texture.

References

[1] M. Ashikhmin, "Synthesizing natural textures," in *Symposium on Interactive 3D Graphics*, 2001, pp. 217–226. [Online]. Available: citeseer.ist.psu.edu/530201.html

[2] J. D. Bonet and P. Viola, *A non-parametric multi-scale statistical model for natural images*. MIT Press, 1997, ch. 9.

[3] S. Boyd, L. E. Ghaoui, E. Feron, and V. Balakrishnan, *Linear Matrix Inequalities in Systems and Control Theory*. Philadelphia: SIAM Studies in Applied Mathematics, 1994.

[4] D. Cano and T. H. Minh, "Texture synthesis using hierarchical linear transforms," *Signal Processing*, vol. 15, pp. 131–148, 1988.

[5] R. Chellappa and R. Kashyap, "Texture synthesis using 2d noncausal autoregressive models," *IEEE Trans. on Acoustics, Speech and Signal Processing*, vol. assp-33, no. 1, pp. 194–199, February 1985.

[6] G. R. Cross and A. K. Jain, "Markov random field texture models," *IEEE Trans. on Pattern Analysis and Machine Intelligence*, vol. 5, pp. 713–718, 1983.

[7] G. Doretto, A. Chiuso, Y. N. Wu, and S. Soatto, "Dynamic textures," *Int. J. Computer Vision*, vol. 51, no. 2, pp. 91–109, 2003.

[8] A. Efros and T. Leung, "Texture synthesis by non-parametric sampling," in *ICCV*, 1999.

[9] A. A. Efros and W. T. Freeman, "Image quilting for texture synthesis and transfer," in *Proceedings of the 28th annual conference on Computer graphics and interactive techniques*. ACM Press, 2001, pp. 341–346.

[10] S. Geman and D. Geman, "Stochastic relaxation, gibbs distributions and the bayesian restoration of images," *IEEE Trans. on Pattern Analysis and Machine Intelligence*, vol. 6, pp. 721–741, 1984.

[11] L. V. Gool, P. Dewaele, and A. Oosterlinck, "Survey: texture analysis anno," *cvgip*, vol. 29, pp. 336–357, 1985.

[12] R. M. Haralick, "Statistics and structural approach to texture," *Proc. IEEE*, vol. 67, pp. 786–804, 1979.

[13] P. Harrison, "A non-hierarchical procedure for re-synthesis of complex textures," in *WSGC*, 2001, pp. 190–197.

[14] D. Heeger and J. Bergen, "Pyramid-based texture analysis/synthesis," in *ACM SIGGRAPH*, 1995.

[15] B. Julesz, "Visual pattern discrimination," *IRE Trans. of Information Theory*, vol. IT, no. 8, pp. 84–92, 1962.

[16] H. C. Lin, L. L. Wang, and S. N. Yang, "Extracting periodicity of a regular texture based on autocorrelation functions," *Pattern Recognition Letters*, vol. 18, p. 433443, 1997.

[17] Y. Liu, R. Collins, and Y. Tsin, "A computational model for periodic pattern perception based on frieze and wallpaper groups," *IEEE Transactions on Pattern Analysis and Machine Intelligence*, vol. 26, no. 3, pp. 354 – 371, March 2004.

[18] J. Mao and A. K. Jain, "Texture classification and segmentation using multiresolution simultaneous autoregressive models," *Pattern Recognition*, vol. 25, pp. 173–188, 1992.

[19] L. Mirsky, "Symmetric gauge functions and unitarily invariant norms," *Quartely J. of Mathematics*, vol. 11, pp. 50–59, 1960.

[20] T. Ojala, M. Pietikainen, and D. Hardwood, "A comparative study of texture measures with classification based on feature distributions," *Pattern Recognition*, vol. 29, no. 1, pp. 51–59, 1996.

[21] K. Popat and R. W. Picard, "Cluster-based probability model and its application to image and texture processing," *IEEE Trans. on Image Processing*, vol. 6, no. 2, pp. 268–284, 1997.

[22] M. Porat and Y. Y. Zeevi, "Localized texture processing in vision: Analysis and synthesis in gaborian space," *IEEE Trans. Biomedical Engineering*, vol. 36, no. 1, pp. 115–129, 1989.

[23] J. Portilla and E. P. Simoncelli, "A parametric texture model based on joint statistics of complex wavelet coefficients," *Int. Journal of Computer Vision*, vol. 40, no. 1, pp. 49–71, 2000.

[24] T. Randen and J. H. Husoy, "Filtering for texture classificatiob: A comparative study," *pami*, vol. 21, no. 4, pp. 291–310, 1999.
[25] S. D. Rane, G. Sapiro, and M. Bertalmio, "Structure and texture filling-in of missing image blocks in wireless transmission and compression appications," *ip*, vol. 12, no. 3, pp. 296–303, March 2003.
[26] M. Tuceryan and A. K. Jain, "Texture analysis," in *Handbook of Pattern Recognition and Computer Vision*, . H. Chen, L. F. Pau, and P. S. P. Wang, Eds. World Science Publishing, 1993, pp. 235–276.
[27] L. Y. Wei and M. Levoy, "Order-independent texture synthesis," Standford University, Computer Science Department, Tech. Rep. TR-2002-01, April 2002.
[28] Y. Q. Xu, B. Guo, and H. Shum, "Chaos mosaic: Fast and memory efficient texture synthesis," Microsoft Research, Tech. Rep. MSR-TR-2000-32, April 2000.
[29] J. Yuan and S. T. Rao, "Spectral estimation for random fields with applications to markov modeling and texture classification," in *Markov random Fields*, Chellappa and Jain, Eds., 1993.
[30] J. Zhang and T. Tan, "Brief review of invariant texture analysis methods," *Pattern Recognition*, vol. 35, pp. 735–747, 2002.
[31] S. C. Zhu, Y. Wu, and D. Mumford, "Filters, random fields and maximum entropy (FRAME): towards a unified theory for texture modeling," *Int. Journal of Computer Vision*, vol. 27, no. 2, pp. 107–126, 1998.

APPENDIX

A. Proof of Theorem 1

In order to prove Theorem 1 we need the following preliminary result:

Lemma 1: Consider the singular value decomposition of a matrix $\mathbf{H} \in \mathcal{H}$:

$$\mathbf{H} = \begin{bmatrix}\mathbf{U}_r & \mathbf{U}_{n-r} & \mathbf{U}_\perp\end{bmatrix} \begin{bmatrix}\mathbf{S}_r & \mathbf{0} & \mathbf{0}\\ \mathbf{0} & \mathbf{S}_{n-r} & \mathbf{0}\\ \mathbf{0} & \mathbf{0} & \mathbf{0}\end{bmatrix} \begin{bmatrix}\mathbf{V}_r^T\\ \mathbf{V}_{n-r}^T\\ \mathbf{V}_\perp^T\end{bmatrix}.$$

If $\sigma_r > \sigma_{r+1}$ then $\mathbf{P}_L\mathbf{U}_r \in$ span colums$(\mathbf{U}_r)$.

Proof: Let

$$\mathbf{P}_R = \begin{bmatrix} 0 & \mathbf{I}_m & 0 & \dots & 0\\ 0 & 0 & \mathbf{I}_m & \dots & 0\\ \vdots & \vdots & \ddots & \vdots & \\ \mathbf{I}_m & 0 & 0 & \dots & 0\end{bmatrix} \quad (23)$$

It can be easily verified that $\mathbf{P}_L\mathbf{H}\mathbf{P}_R = \mathbf{H}$. Thus, for any left eigenvector $\mathbf{u}^T$ of $\mathbf{H}\mathbf{H}^T$ we have:

$$\begin{aligned}&\mathbf{u}^T\mathbf{H}\mathbf{H}^T = \sigma\mathbf{u}^T \Rightarrow \mathbf{u}^T\mathbf{H}\mathbf{H}^T\mathbf{P}_L^T = \sigma\mathbf{u}^T\mathbf{P}_L^T \Rightarrow\\ &\mathbf{u}^T\mathbf{P}_L^T\mathbf{P}_L\mathbf{H}\mathbf{P}_R\mathbf{P}_R^T\mathbf{H}^T\mathbf{P}_L^T = \sigma\mathbf{u}^T\mathbf{P}_L^T \Rightarrow\\ &\mathbf{u}^T\mathbf{P}_L^T\mathbf{H}\mathbf{H}^T = \sigma\mathbf{u}^T\mathbf{P}_L^T\end{aligned} \quad (24)$$

where we used the facts that $\mathbf{P}_L^T\mathbf{P}_L = \mathbf{I}$ and $\mathbf{P}_R\mathbf{P}_R^T = \mathbf{I}$. From the last equation it follows that $\mathbf{u}^T\mathbf{P}_L^T$ is also an eigenvector of $\mathbf{H}\mathbf{H}^T$, with eigenvalue σ. The proof follows now from the facts that subspaces corresponding to different eigenvalues of $\mathbf{H}\mathbf{H}^T$ are orthogonal and that the condition $\sigma_r > \sigma_{r+1}$ guarantees that the subspaces spanned by the columns of $\mathbf{U}_r$ and $\mathbf{U}_{n-r}$ are orthogonal. ■

The proof of *Theorem 1* is given next:

Proof: *Property (i):* Start by partitioning $\mathbf{U} = [\mathbf{U}_r \quad \mathbf{U}_{n-r} \quad \mathbf{U}_\perp]$. Since $\mathbf{P}_L\mathbf{U}_r$ is orthogonal to $[\mathbf{U}_{n-r} \quad \mathbf{U}_\perp]$, it follows that $\mathbf{U}_r\mathbf{U}_r^T\mathbf{P}_L\mathbf{U}_r = \left(\mathbf{I} - \mathbf{U}_{n-r}\mathbf{U}_{n-r}^T - \mathbf{U}_\perp^T\mathbf{U}_\perp\right)\mathbf{P}_L\mathbf{U}_r = \mathbf{P}_L\mathbf{U}_r$. Thus $\mathbf{A}_r^k = \mathbf{S}_r^{\frac{-1}{2}}\mathbf{U}_r^T\mathbf{P}_L^k\mathbf{U}_r\mathbf{S}_r^{\frac{1}{2}}$. The fact that $\mathbf{A}^n = I$ follows directly from $\mathbf{P}_L^n = I$.

Property (ii): Start by defining:

$$\begin{aligned}&\mathbf{E}_L^{(k)} \doteq [\underbrace{\mathbf{0}\dots\mathbf{0}}_{k-1}\mathbf{I}_p\dots\mathbf{0}],\ \mathbf{E}_R^{(k)} \doteq [\underbrace{\mathbf{0}\dots\mathbf{0}}_{k-1}\mathbf{I}_m\dots\mathbf{0}]^T\\ &\mathbf{h}_{ij} \in R^{p\times m} = \mathbf{E}_L^{(i)}\mathbf{H}\mathbf{E}_R^{(j)}\end{aligned}$$

and use the expressions for $\mathbf{C}_r, \mathbf{B}_r$ and $\mathbf{A}_r^k$ to compute $\mathbf{C}_r\mathbf{A}_r^{k-1}\mathbf{B}_r$ leading to:

$$\begin{aligned}&\mathbf{C}_r\mathbf{A}_r^{k-1}\mathbf{B}_r = \mathbf{U}_r^{(1)}\mathbf{U}_r^T\mathbf{P}_L^{k-1}\mathbf{U}_r\mathbf{S}_r\mathbf{V}_r^{(1)}\\ &= \mathbf{E}_L^{(1)}\mathbf{U}_r\mathbf{U}_r^T\mathbf{P}_L^{k-1}\mathbf{U}_r\mathbf{S}_r\mathbf{V}_r^{(1)} = \mathbf{E}_L^{(1)}\mathbf{P}_L^{k-1}\mathbf{U}_r\mathbf{S}_r\mathbf{V}_r\mathbf{E}_R^{(1)}\\ &= \mathbf{E}_L^{(k-1)}\mathbf{H}_r\mathbf{E}_R^{(1)} = \mathbf{h}_{k,1}\end{aligned} \quad (25)$$

Next, compute

$$\begin{aligned}\mathbf{h}_{i,j} &= \mathbf{E}_L^{(i)}\mathbf{H}_r\mathbf{E}_R^j = \mathbf{E}_L^{(1)}\mathbf{P}_L^{(i-1)}\mathbf{H}_r\mathbf{P}_R^{-(j-1)}\mathbf{E}_R^{(1)}\\ &= \mathbf{E}_L^{(1)}\mathbf{P}_L^{i+j-2}\mathbf{P}_L^{-(j-1)}\mathbf{H}_r\mathbf{P}_R^{-(j-1)}\mathbf{E}_R^{(1)}\\ &= \mathbf{E}_L^{(i+j-2)}\mathbf{H}_r\mathbf{E}_R^{(1)} = \mathbf{h}_{i+j-2,1}\end{aligned}$$

Thus, $\mathbf{H}_r = (\mathbf{h}_{i,j})$ has the required block circulant Hankel structure. Since by construction $\mathbf{Y}$ is also a block circulant Hankel matrix, it follows that $\mathbf{H}_\mathbf{e} \doteq \mathbf{Y} - \mathbf{H}_r$ has a block circulant Hankel structure. Moreover, from (10), it follows that

$$\mathbf{H}_\mathbf{e} = \begin{bmatrix}\mathbf{U}_r & \mathbf{U}_{n-r} & \mathbf{U}_\perp\end{bmatrix} \begin{bmatrix}\mathbf{0} & \mathbf{0} & \mathbf{0}\\ \mathbf{0} & \mathbf{S}_{n-r} & \mathbf{0}\\ \mathbf{0} & \mathbf{0} & \mathbf{0}\end{bmatrix} \begin{bmatrix}\mathbf{V}_r^T\\ \mathbf{V}_{n-r}^T\\ \mathbf{V}_\perp^T\end{bmatrix}$$

where $\mathbf{S}_{n-r} = \text{diag}\{\sigma_{r+1},\dots,\sigma_n\}$. This, together with (9) implies that $\bar{\sigma}(\mathbf{H}_\mathbf{e}) \le \epsilon$. Thus, from (7) we have that:

$$\begin{aligned}\mathbf{Y} = \mathbf{H}_\mathcal{I}\mathbf{H}_u^T = \mathbf{H}_r + \mathbf{H}_\mathbf{e} \Rightarrow\\ \mathbf{H}_\mathcal{I} = \mathbf{H}_r\mathbf{H}_u + \mathbf{H}_\mathbf{v}\end{aligned} \quad (26)$$

where we defined $\mathbf{H}_\mathbf{v} \doteq \mathbf{H}_\mathbf{e}\mathbf{H}_u$. Note that since $\mathbf{H}_u$ is unitary, then $\bar{\sigma}(\mathbf{H}_\mathbf{v}) \le \epsilon$. From the first column of the (matrix) equation (26) it follows that:

$$\mathbf{R}_k^T = \sum_{i=1}^{n}\mathbf{C}\mathbf{A}^{k-i}\mathbf{B}u_i + \mathbf{v}_k$$

with $u_i \doteq \mathbf{H}_u(i,1)$ and $\mathbf{v}_k \doteq \mathbf{H}_\mathbf{v}(k,1)$. ■

Corollary 1: Given $\mathbf{Y} \in \mathcal{H}^n$, consider the following constrained approximation problem:

$$\mu_c \doteq \min_{\mathbf{H}_r}\bar{\sigma}(\mathbf{Y} - \mathbf{H}_r) \text{ subject to} \begin{cases}\text{rank}(\mathbf{H}_r) \le r\\ \mathbf{H}_r \in \mathcal{H}^n\end{cases} \quad (27)$$

Then the minimizing $\mathbf{H}_r$ is given by (10) and $\mu_c = \sigma_{r+1}$.

Proof: By construction (Mirsky's Theorem [19]), $\mathbf{H}_r$ solves the rank-constrained approximation problem

$$\mu_{uc} \doteq \min_{\mathbf{H}_r}\bar{\sigma}(\mathbf{Y} - \mathbf{H}_r) \text{ subject to rank}(\mathbf{H}_r) \le r.$$

The fact that $\mathbf{H}_r$ solves (27) follows from the fact that in general $\mu_{uc} \le \mu_c$ with $\mathbf{H}_r$ achieving equality in this case. ■